Electric-field-induced magnetic easy-axis reorientation in ferromagnetic/ferroelectric layered heterostructures

Jia-Mian Hu and C. W. Nan*
Department of Materials Science and Engineering, State Key Laboratory of New Ceramics and Fine Processing, Tsinghua University, Beijing 100084, China

(Received 15 September 2009; revised manuscript received 20 November 2009; published 16 December 2009)

A phenomenological model is presented for the *electric-field-induced* reorientation of magnetic easy axis in ferromagnetic (FM)/ferroelectric (FE) layered heterostructures, where the FM layers include either polycrystalline or (001) preferentially oriented films of widely used Fe, $CoFe_2O_4$ (CFO), Ni, and Fe_3O_4. The magnetic easy axes could rotate within the film plane at relatively low applied electric fields in CFO, Ni, and Fe_3O_4 films. As the applied electric field increases, the easy axes tend to switch from an in-plane direction to an out-of-plane one in CFO and Ni films. Such electric-field-induced easy-axis reorientations (EARs) can be abrupt and gradual, defined as first-order and second-order transitions, respectively. The influences of residual strain, different electric-field orientations, and nonlinear strain vs electric-field behavior of the FE substrates, on the EARs are also addressed.

DOI: 10.1103/PhysRevB.80.224416 PACS number(s): 75.80.+q, 75.30.Gw, 77.80.Fm, 77.84.Lf

I. INTRODUCTION

Magnetoelectric (ME) coupling in composite materials with two ferroic components (e.g., ferroelectric and ferromagnetic), resulting from the cross interaction between different ordering of the two ferroic phases, has been under intensive study recently.[1] Given that their electric and magnetic properties are coupled, it becomes possible to control the magnetization (or electric polarization) by applying an electric (or magnetic) field alone. Among them, the electric-field control of magnetization is particularly appealing, owing to its potential applications in novel ME devices such as electric-write magnetic memories[2] and electrically tunable microwave magnetic devices.[3] In the electric-write magnetic memory case, the electric field is used to switch the magnetic easy axis (or easy plane) to a certain direction in which the data recording is favored.

The electric-field control of magnetic anisotropy in ME composites, which is essentially a converse ME effect (i.e., a change in magnetization M due to an applied electric field E),[1,4] has been observed experimentally in heterostructures such as a heterostructure of ferromagnetic thin film and intrinsically multiferroic $BiFeO_3$,[5] and diluted magnetic semiconductors using field effects.[6,7] Another attractive approach for the electric-field control of magnetization at room temperature takes advantage of the strain-mediated ME coupling in multiferroic composites such as heterostructures with ferromagnetic (FM) films grown on ferroelectric (FE) substrates.[4,8–10] The *room-temperature* switching of magnetic easy axis in such FM/FE heterostructures is usually more remarkable due to the relatively strong strain-mediated ME coupling, compared to the direct coupling at room temperature in current most single-phase multiferroics where dramatic ME behaviors were normally observed only at very low temperature.[2]

In addition, the electric-field modification in magnetization could also occur by interfacial chemical bonding[11] or the accumulation of spin-polarized screening charges at the interface,[12] based on recent first-principle density-functional calculations. However, in FM/FE heterostructures, elastic strains play a very important role in the ME coupling.[13] Such strain-mediated ME coupling could result in a rotation of magnetic easy axis, namely, the strain-induced easy-axis reorientations (EARs). Recently, Pertsev[14] has calculated the EARs at *moderate strain* in (001)-oriented $CoFe_2O_4$ (CFO) and Ni films grown on relaxor ferroelectrics such as $Pb(Zn_{1/3}Nb_{2/3})O_3$-$PbTiO_3$ (PZN-PT) or $Pb(Mn_{1/3}Nb_{2/3})O_3$-$PbTiO_3$, using a phenomenological approach.[15–17] It was considered that lattice misfit at the FM/FE interface or an electric field applied to the FE substrate could cause the strain-induced out-of-plane EAR, i.e., the strain-induced switching of magnetic easy axis from an in-plane direction to an out-of-plane one (or vise versa).[14] Such an out-of-plane EAR has great technological potentials in the prototypical electric-field-assisted magnetic recording devices. In addition to this important out-of-pane EAR which will be discussed in details for more material systems in the present paper, the electric field could more easily generate an in-plane EAR where the magnetic easy axis just rotates within the film plane, which has been verified in recent experimental observations.[9,10] This *electric-field-induced* in-plane EAR will be also illustrated in the present paper.

In this paper, we present a detailed discussion on the electric-field-induced EARs in FM/FE-layered heterostructures, based on a phenomenological approach, with various magnetic films (e.g., Fe, CFO, Ni, and Fe_3O_4) grown on FE substrates [e.g. PZN-PT, $BaTiO_3$ (BTO), and $Pb(Zr,Ti)O_3$ (PZT)]. The influence of the residual strains as well as different modes of applied electric fields on the EARs is studied. After introducing the phenomenological anisotropy model used for calculation in Sec. II, two different kinds of electric-field-induced EARs (i.e., out-of-plane and in-plane EARs) in (001)-oriented and polycrystalline magnetic films are discussed in Secs. III and IV, respectively. The effect of nonlinear strain vs electric-field behavior of the FE substrate on the out-of-plane EAR is addressed in Sec. III. The conclusions are summarized in Sec. V.

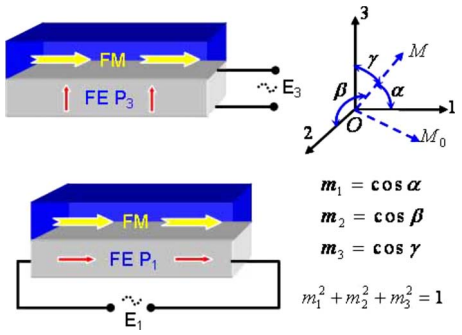

FIG. 1. (Color online) FM/FE heterostructure used in the model. The arrows denote the orientation of magnetization (polarization) in the FM (FE) layer. An out-of-plane polarization P_3 or in-plane polarization P_1 can be generated by an external electric field applied along the out-of-plane (i.e., longitudinal electric field E_3) or in-plane (i.e., transverse electric-field E_1) direction. Vector diagram of an out-of-plane EAR from $\overrightarrow{OM}_0$ to $\overrightarrow{OM}$ is shown on the right-hand side of the panel.

II. ANISOTROPY MODEL

Consider a FM/FE bilayered heterostructure with a FM film grown on a FE substrate. In the FE substrate, the out-of-plane polarization P_3 or in-plane polarization P_1 can be generated by an external electric field applied along the out-of-plane (i.e., longitudinal electric field E_3) or in-plane (i.e., transverse electric-field E_1) direction, respectively, as shown in Fig. 1. The in-plane strains are caused by the electric fields in both cases through the converse piezoelectric effect. The FM films grown on FE substrates could be polycrystalline or epitaxial, depending on the deposition processing. For a polycrystalline FM film, single grains at the bottom of the FM film could make a coherent epitaxial relation to the FE substrate. We assume a perfect interface where the piezostrains generated by the FE substrate could be fully transferred to the FM film.

In general, the total anisotropy energy of a FM film can be described as the sum of magnetocrystalline anisotropy energy F_{mc}, magnetostatic energy F_{ms} (including shape anisotropy F_{shape} and exchange anisotropy F_{ex}), and magnetoelastic energy F_{me}.[15] For the FM films in a single-domain state, the total free energy F_{tot} could be written as

$$F_{tot} = F_{mc} + F_{shape} + F_{me} \tag{1}$$

with exchange anisotropy between domains being neglected. In the previous model,[14] the pure elastic energy F_{el} was included in the total free energy. However in our model, it is just used to derive the mechanical equilibrium conditions as discussed below, which is more reasonable. When the spontaneous magnetization (magnetic easy axis) rotates from its initial in-plane direction $\overrightarrow{OM}_0$ to another direction along $\overrightarrow{OM}$ (see Fig. 1), the change in the total free energy is

$$\Delta F_{tot} = F_M - F_{M_0} = \Delta F_{mc} + \Delta F_{shape} + \Delta F_{me}. \tag{2}$$

If $\Delta F_{tot} < 0$, the orientation $\overrightarrow{OM}$ is energetically more favorable, i.e., this rotation can happen.

First, let us consider the change in the magnetocrystalline anisotropy energy ΔF_{mc}. For an epitaxial cubic ferromagnetic film, ΔF_{mc} can be written as

$$\Delta F_{mc} = F_{mc}^{M} - F_{mc}^{M_O} = K_1(m_1^2m_2^2 + m_1^2m_3^2 + m_2^2m_3^2) + K_2m_1^2m_2^2m_3^2, \tag{3}$$

where K_i and m_i $(i=1,2,3)$ are the bulk anisotropy constants and the direction cosines of the magnetic easy axis with respect to the principal cubic axis (see Fig. 1), respectively. As to polycrystalline films with randomly oriented grains, $\overrightarrow{OM}_0$ and $\overrightarrow{OM}$ are two cystallographically equivalent directions, which means $\Delta F_{mc}=0$, and thus it does not contribute to ΔF_{tot}.

The shape anisotropy change in both polycrystalline and epitaxial films can be written as

$$\Delta F_{shape} = F_{shape}^{M} - F_{shape}^{M_O} = \frac{1}{2}\mu_0 M_S^2 m_3^2, \tag{4}$$

which is a positive-energy contribution, favoring magnetic easy axis to lie in the film plane.

The magnetoelastic energy reflects the coupling between the magnetization and elastic strains, and its change ΔF_{me} can be expressed as

$$\Delta F_{me} = B_1\left[\left(m_1^2 - \frac{1}{3}\right)\varepsilon_{11} + \left(m_2^2 - \frac{1}{3}\right)\varepsilon_{22} + \left(m_3^2 - \frac{1}{3}\right)\varepsilon_{33}\right] + B_2(m_1m_2\varepsilon_{12} + m_1m_3\varepsilon_{13} + m_2m_3\varepsilon_{23}), \tag{5}$$

where B_1 and B_2 are magnetoelastic coupling coefficients, and ε_{ij} (i and $j=1,2,3$) are the elastic strains defined in the crystallographic reference frame,[15] which is the same as the principal crystal axes for (001)-oriented epitaxial systems. Furthermore, B_1 and B_2 can be described by the magnetostrictive constants, λ_{100} and λ_{111}, of the FM films,[18] i.e.,

$$B_1 = -\frac{3}{2}\lambda_{100}(c_{11} - c_{12}),$$

$$B_2 = -3\lambda_{111}c_{44} \tag{6}$$

for epitaxial FM films and

$$B_1 = -\frac{3}{2}\lambda_S(c_{11} - c_{12}), \quad B_2 = -3\lambda_S c_{44},$$

$$\lambda_{100} = \lambda_{111} = \lambda_S \tag{7}$$

for polycrystalline FM films. Here c_{11}, c_{12}, and c_{44} are the elastic stiffness constants of the cubic FM films. From Eq. (5), it can be seen that the magnetoelastic energy depends linearly on the elastic strains ε_{ij}. In this case, a crystal would undergo an unrestricted deformation with increasing anisotropy energy, which is not possible. Therefore, an extra energy term for balance, i.e., the elastic contribution F_{el}, should be involved to calculate the elastic strains ε_{ij} in mechanical equilibrium, and its change ΔF_{el} equals

$$\Delta F_{el} = \frac{1}{2}c_{11}(\varepsilon_{11}^2 + \varepsilon_{22}^2 + \varepsilon_{33}^2) + c_{12}(\varepsilon_{11}\varepsilon_{22} + \varepsilon_{11}\varepsilon_{33} + \varepsilon_{22}\varepsilon_{33}) + \frac{1}{2}c_{44}(\varepsilon_{12}^2 + \varepsilon_{13}^2 + \varepsilon_{23}^2). \quad (8)$$

Since the heterostructures is mechanically free on the upper surface, the out-of-plane stresses should be zero, i.e., $\sigma_{13}=\sigma_{23}=\sigma_{33}=0$. Then the elastic strains ε_{13}, ε_{23}, and ε_{33} in Eqs. (5) and (8) could be deduced according to the mechanical equilibrium equation $\sigma_{ij}=\partial(\Delta F_{me}+\Delta F_{el})/\partial\varepsilon_{ij}$. Assuming that there is no shear deformation at the FM/FE interface, we have

$$\varepsilon_{33} = -\left[B_1\left(m_3^2 - \frac{1}{3}\right) + c_{12}(\varepsilon_{11}+\varepsilon_{22})\right]/c_{11},$$

$$\varepsilon_{12}=0, \quad \varepsilon_{13}=-B_2 m_1 m_3/c_{44}, \quad \varepsilon_{23}=-B_2 m_2 m_3/c_{44}. \quad (9)$$

By considering a perfect interface, the in-plane elastic strains generated by the FE layer can then be mediated to the upper FM film homogeneously, i.e., $\varepsilon_{11,22}^{\mathrm{FE}}=\varepsilon_{11,22}^{\mathrm{FM}}$. Thus, the relationship between the elastic strains and applied electric field can be expressed as

$$\varepsilon_{11}=\varepsilon_{22}=\varepsilon_0+d_{31}E_3 \quad (10)$$

for a longitudinal electric field E_3 (see Fig. 1) and

$$\varepsilon_{11}=\varepsilon_0+d_{33}E_1,$$

$$\varepsilon_{22}=\varepsilon_0+d_{31}E_1 \quad (11)$$

for a transverse electric field E_1 (see Fig. 1). Here d_{31} and d_{33} are piezoelectric coefficients of the FE layers; and ε_0 denotes the residual strain arising from lattice mismatch or thermal-expansion mismatch between the bilayers during deposition process. It can be seen from Eqs. (10) and (11) that the in-plane piezostrains ε_{11} and ε_{22} are the same under an E_3-field while different both in sign and magnitude under an E_1 field since $d_{33}>0$ and $d_{31}<0$.

The direction cosines m_1 and m_2 in the equations above are assumed to be equal for simplicity. This assumption is reasonable for two cases: (i) polycrystalline FM films exhibit a magnetic easy plane where m_1 and m_2 are geometrically equivalent, and (ii) m_1 and m_2 in (001)-oriented FM films are also deemed to be equal when a longitudinal electric field is applied to the FE substrates due to the same in-plane elastic strains as shown in Eq. (10).

The summation of all these contributions yields the total free-energy change ΔF_{tot} when the easy axis switches from $\widetilde{OM}_0$ to $\widetilde{OM}$, i.e.,

$$\Delta F_{tot} = \left[\frac{K_1}{2}+\frac{K_2}{4}+\frac{1}{2}\mu_0 M_S^2+\frac{2B_1^2}{3c_{11}}-\frac{B_2^2}{c_{44}} - \left(\frac{B_1}{2}+\frac{B_1 c_{12}}{c_{11}}\right)(\varepsilon_{11}+\varepsilon_{22})\right]m_3^2 + \left(\frac{B_2^2}{c_{44}}-\frac{B_1^2}{c_{11}}-\frac{3}{4}K_1-\frac{K_2}{2}\right)m_3^4+\frac{K_2}{4}m_3^6 \quad (12)$$

in cubic epitaxial FM films and

$$\Delta F_{tot} = \left[\frac{1}{2}\mu_0 M_S^2+\frac{2B_1^2}{3c_{11}}-\frac{B_2^2}{c_{44}}-\left(\frac{B_1}{2}+\frac{B_1 c_{12}}{c_{11}}\right)(\varepsilon_{11}+\varepsilon_{22})\right]m_3^2 + \left(\frac{B_2^2}{c_{44}}-\frac{B_1^2}{c_{11}}\right)m_3^4 \quad (13)$$

in cubic polycrystalline FM films. Eqs. (12) and (13) illustrate that the sign and magnitude of ΔF_{tot} depend on the in-plane elastic strains ε_{11} and ε_{22} which are related to the applied electric field by Eqs. (10) and (11). Furthermore, the electric-field-induced EARs can be described through the minimization of ΔF_{tot} with respect to the direction cosine m_3. $m_3=0$ represents an energetically favorable in-plane easy axis while $m_3=1$ indicates an easy axis normal to the film surface.

By combining Eqs. (10)–(13) and minimizing ΔF_{tot} with respect to direction cosine m_3, we can derive the critical electric field E^{cr} required for the EARs, i.e.,

$$E_3^{cr}=\frac{K_A}{2td_{31}}-\frac{\varepsilon_0}{d_{31}},$$

$$E_1^{cr}=\frac{K_A}{t(d_{31}+d_{33})}-\frac{2\varepsilon_0}{(d_{31}+d_{33})}, \quad (14)$$

where E_3^{cr} and E_1^{cr} are the critical electric fields in the E_3 and E_1 modes, and K_A and t are, respectively,

$$K_A = \begin{cases} \dfrac{K_1}{2}+\dfrac{K_2}{4}+\dfrac{1}{2}\mu_0 M_S^2+\dfrac{2B_1^2}{3c_{11}}-\dfrac{B_2^2}{c_{44}}, & \text{for epitaxial case} \\ \dfrac{1}{2}\mu_0 M_S^2+\dfrac{2B_1^2}{3c_{11}}-\dfrac{B_2^2}{c_{44}}, & \text{for polycrystalline case,} \end{cases}$$

$$t=\frac{B_1}{2}+\frac{B_1 c_{12}}{c_{11}}. \quad (15)$$

As $|E|>|E^{cr}|$, the magnetic easy axis would rotate.

Furthermore, ΔF_{tot} of Eqs. (12) and (13) can be simplified by ignoring the high-order term of m_3 as

$$\Delta F_{tot} = \begin{cases} -2td_{31}(E_3-E_3^{cr})m_3^2+K_B m_3^4, & \text{in the } E_3 \text{ mode} \\ -2t(d_{31}+d_{33})(E_1-E_1^{cr})m_3^2+K_B m_3^4, & \text{in the } E_1 \text{ mode} \end{cases} \quad (16)$$

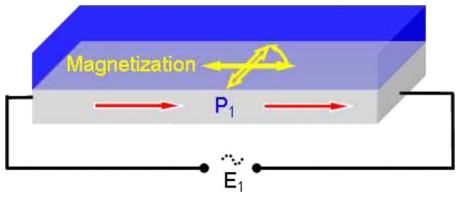

FIG. 2. (Color online) Schematic of an electric-field-induced in-plane EAR by a transverse electric field E_1. The crossed arrows (yellow) in the upper layer and rightward arrows (red) in the bottom layer denote the orientations of magnetization and polarization, respectively.

with

$$K_B = \begin{cases} \frac{B_2^2}{c_{44}} - \frac{B_1^2}{c_{11}} - \frac{3}{4}K_1 - \frac{K_2}{2}, & \text{for epitaxial case} \\ \frac{B_2^2}{c_{44}} - \frac{B_1^2}{c_{11}}, & \text{for polycrystalline case.} \end{cases} \tag{17}$$

In Eq. (16), the direction cosine m_3, which shows the orientation of the magnetization (magnetic easy axis), behaves like an order parameter. As discussed in the following sections, a gradual electric-field-induced EAR will take place when the *quartic coefficient* $K_B>0$, where m_3 changes continuously from zero at $E=E^{cr}$ to one. On the other hand, an abrupt electric-field-induced EAR will happen when $K_B<0$, where m_3 changes discontinuously from zero to one at $E=E^{cr}$. In that respect, we can define a second-order (continuous) electric-field-induced EAR as $K_B>0$ and a first-order (abrupt) electric-field-induced EAR as $K_B<0$.

Here we classify the reorientation of the magnetic easy axis into two categories. The first is an out-of-plane EAR, which means the magnetic easy axis switches from the initial in-plane direction $\overrightarrow{OM}_0$ to a direction $\overrightarrow{OM}$ off the plane (see Fig. 1). The other is called an in-plane EAR, where the magnetic easy axis rotates within the film plane (see Fig. 2). For the out-of-plane EAR, all energy contributions discussed above are taken into account. Whereas in the case of the in-plane EAR, the large out-of-plane shape anisotropy can be omitted. For illustration, the calculations were performed for iron (Fe), CFO, nickel (Ni), and magnetite (Fe_3O_4) films, respectively. The materials parameters of these FM films used for numerical calculations are shown in Table I. The FE layers in our model include relaxor ferroelectrics such as PZN-PT with ultrahigh piezoelectric coefficients ($d_{33}\sim 2500$ pm/V and $d_{31}\sim -1100$ pm/V) (Refs. 19 and 20) and normal ferroelectrics such as BTO ($d_{33}\sim 190$ pm/V and $d_{31}\sim -78$ pm/V) (Ref. 21) or PZT ($d_{33}\sim 410$ pm/V and $d_{31}\sim -170$ pm/V).[22]

III. ELECTRIC-FIELD-INDUCED OUT-OF-PLANE EAR

A. (001)-oriented and polycrystalline Fe films

Figure 3 shows the electric-field-induced out-of-plane EAR in Fe films. The stable orientation of the magnetic easy axis, shown by the direction cosine m_3, is determined by finding the minima of the total free energy ΔF_{tot} [e.g., see Fig. 3(a)]. It can be seen that the magnetic easy axis of the (001) Fe films lies in the film plane ($m_3=0$) under zero electric field when no residual strain ($\varepsilon_0=0$) is taken into account but that a longitudinal electric field of $E_3=3$ MV/cm can turn the easy axis to the direction normal to the film plane ($m_3=1$). The critical fields E^{cr} in the E_3 and E_1 modes for such electric-field-induced out-of-plane EAR are given in Fig. 3(b), where the FE layer is PZN-PT and the residual strain ε_0 is neglected. As the applied electric field reaches the critical one, the electric-field-induced out-of-plane EAR suddenly happens, i.e., a first-order EAR transition happens since the *quartic coefficient* K_B for (001) Fe film is negative (about -35568 J/m^3). Both the sign and magnitude of E_3^{cr} and E_1^{cr} are different according to Eq. (14). As the magnetostrictive constant λ_{100} of the (001) Fe film is positive (see Table I), a negative total in-plane strain $\varepsilon_{tot}=\varepsilon_{11}+\varepsilon_{22}$ is thus needed to switch the easy axis to the out of plane. Therefore, E_3^{cr} and E_1^{cr} should be positive and negative by Eqs. (10) and (11), respectively, as shown in Fig. 3(b). The magnitude of E_3^{cr} is smaller than that of E_1^{cr}, indicating that the electric-field-induced out-of-plane EAR is more likely to happen in the E_3 mode due to the larger total in-plane strain ε_{tot} generated in the E_3 mode. As seen from Eq. (14), ε_0 also has an effect on the critical electric field [Fig. 3(d)]. Figure 3(d) shows that both E_3^{cr} and E_1^{cr} decrease with a negative increasing ε_0 whereas increase with a positive increasing ε_0.

In comparison with the (001)-oriented Fe film, the polycrystalline Fe film also exhibits similar electric-field-induced out-of-plane EAR but different critical electric fields as shown in Fig. 3(c). The out-of-plane EAR in the polycrystalline Fe film requires much higher electric fields. The difference is that the magnetostrictive constant λ_S of the polycrystalline Fe film is negative and smaller than λ_{100} of the (001) Fe film as well. Therefore, a larger positive in-plane total strain ε_{tot} is required, leading to a negative E_3^{cr} and positive E_1^{cr}, both with much larger values.

TABLE I. Materials Parameters, i.e., stiffness coefficient c_{ij} (GPa), magnetocystalline coefficients K_i (MJ/m^3), magnetoelastic coupling coefficients B_i (MJ/m^3), magnetostrictive constant λ (ppm), saturation magnetization M_S (10^5 A/m), for iron (Fe), cobalt ferrite (CFO), nickel (Ni), and magnetite (Fe_3O_4), used for the present numerical calculations.

Materials	Fe	CFO	Ni	Fe_3O_4
c_{11}	229	286	246.5	273
c_{12}	134	173	147.3	106
c_{44}	115	97	124.7	97
K_1	0.048	0.1	−0.0045	−0.01
K_2	0.0001		−0.0023	
B_1	−3.43		9.2	
B_2	7.83		10.2	
λ_{100}	24.1	−590		−19.5
λ_{110}		−60		57.1
λ_{111}	−22.7	120		77.6
λ_S	−7	−110	−32.9	35
M_S	17	3.5	4.85	4.78

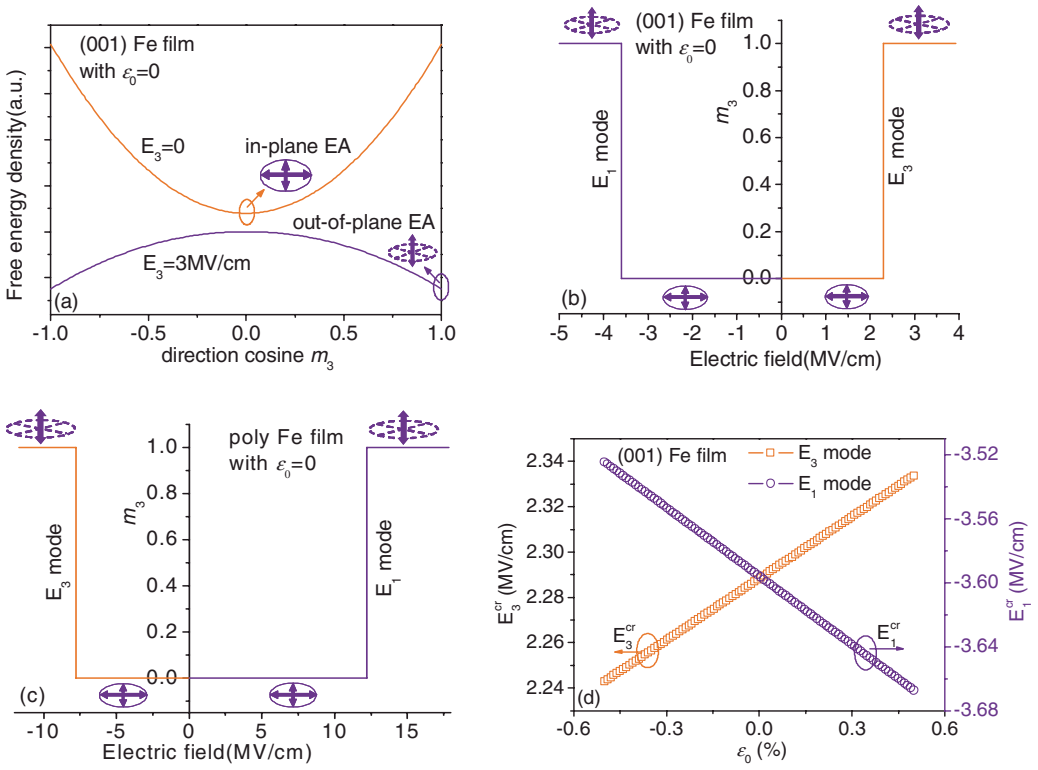

FIG. 3. (Color online) (a) Free energy of (001)-oriented Fe films as a function of the direction cosine m_3 at E_3=0 and E_3=3 MV/cm. Direction cosine m_3 of the magnetic easy axis in (b) (001)-oriented and (c) polycrystalline Fe films as a function of the electric field in the E_3 and E_1 modes at ε_0=0. (d) Dependence of E^{cr} on ε_0 in the E_3 and E_1 modes in (001)-oriented Fe films. The FE layer is PZN-PT. The arrows within ellipses denote the magnetic easy axis.

Tables II and III summarize the critical electric fields required for the electric-field-induced out-of-plane EARs in the (001) and polycrystalline Fe films, respectively, with different FE layers (e.g., PZN-PT, BTO, and PZT) being involved. As shown in Table II and Fig. 3, the critical electric fields E_3^{cr} and E_1^{cr} are far greater than the dielectric breakdown field [i.e., $E_b \sim 0.12$ MV/cm (Ref. 19)] for the FE layers, which makes it experimentally inaccessible. Thus, in the Fe films grown on the FE layers, the strain-mediated ME coupling can not lead to electric-field-induced switching of the magnetic easy axis from an in-plane direction (m_3=0) to an out-of-plane direction (m_3=1). This conclusion is in accordance with Pertsev's which pointed out the out-of-plane EAR in (001)-oriented Fe films could only happen at a *larger* strain than 20% thus inaccessible experimentally.[14]

B. (001)-oriented and polycrystalline CFO films

In (001) CFO films, an abrupt (i.e., a first-order) electric-field-induced out-of-plane EAR takes place [see Fig. 4(a)] due to its negative K_B (i.e., about −97397 J/cm^3) as in the (001) Fe films (Fig. 3). Pertsev[14] also pointed out an abrupt electric-field-induced out-of-plane EAR in (001) CFO film. The critical electric fields E_3^{cr} and E_1^{cr} are negative and positive as ε_0=0, respectively, also determined by a positive critical total in-plane strain ε_{tot} which is further due to the negative λ_{100} of the (001) CFO films. Figure 4(b) shows the ε_0 dependence of the critical electric fields for the (001) CFO films which can also be described by Eq. (14). As seen, both E_3^{cr} and E_1^{cr} increase when ε_0 is negative, and decrease when ε_0 is positive until these critical fields reach zero at a critical EAR point where ε_0 is about 0.06%. After that, both E_3^{cr} and

TABLE II. The critical electric fields E^{cr} for electric-field-induced out-of-plane EAR in the (001) preferentially oriented FM films at ε_0=0 with PZN-PT, BTO, and PZT as the FE layers.

	E_3^{cr} (MV/cm)			E_1^{cr} (MV/cm)		
Films	PZN-PT	BTO	PZT	PZN-PT	BTO	PZT
Fe	2.29	32.27	14.81	−3.6	−44.95	−20.98
CFO	−0.0057	−0.0799	−0.0367	0.0089	0.1113	0.0520
Ni	−0.0650	−0.9165	−0.4205	0.1021	1.277	0.5957
Fe_3O_4	−0.1392	−1.96	−0.9	0.2187	2.73	1.28

TABLE III. The critical electric fields E_1^{cr} for the electric-field-induced out-of-plane EAR in the polycrystalline FM films at $\varepsilon_0=0$ with PZN-PT, BTO, and PZT as the FE layers.

	E_3^{cr} (MV/cm)			E_1^{cr} (MV/cm)		
Films	PZN-PT	BTO	PZT	PZN-PT	BTO	PZT
Fe	−7.77	−109.55	−50.27	12.20	152.59	71.21
CFO	−0.0148	−0.2092	−0.0960	0.0233	0.2913	0.1360
Ni	−0.1241	−1.7495	−0.8027	0.1950	2.4368	1.1372
Fe_3O_4	0.0833	0.1170	0.54	−0.1309	−1.64	−0.76

E_1^{cr} have a sign change and increase with increasing ε_0. Hence, a positive residual strain greater than 0.06% alone can rotate the magnetic easy axis to the out-of-plane direction. This critical residual strain for the out-of-plane EAR is relatively small and can be easily achieved in a film-on-substrate geometry either by lattice misfit or by thermal-expansion misfit during deposition. The orientations of the magnetic easy axes can thus be controlled, which has been verified by recent experimental observation.[23]

Compared to the (001) CFO film, the polycrystalline CFO film presents different behavior of the electric-field-induced out-of-plane EAR. As shown in Fig. 4(c), as the applied electric field E_3 (E_1) reaches E_3^{cr} (E_1^{cr}), the magnetic easy axis does not abruptly switch from an in-plane direction to an out-of-plane one but gradually rotates off the film plane ($0<m_3<1$) and finally orients normal to the film plane ($m_3=1$) until E_3 (E_1) reaches a saturated electric field E_3^S (E_1^S), which denotes the completion of this out-of-plane EAR. Thus a second-order out-of-plane EAR happens due to its positive K_B (i.e., about 9348 J/cm^3). The saturated electric field E_3^S (E_1^S) can be obtained as

$$E_3^S = \frac{K_A + 2K_B}{2td_{31}} - \frac{\varepsilon_0}{d_{31}},$$

$$E_1^S = \frac{K_A + 2K_B}{t(d_{31}+d_{33})} - \frac{2\varepsilon_0}{(d_{31}+d_{33})}. \quad (18)$$

Comparison of Eqs. (14) and (18) gives

$$\Delta E_3^{cr} = E_3^S - E_3^{cr} = \frac{2K_B}{2td_{31}},$$

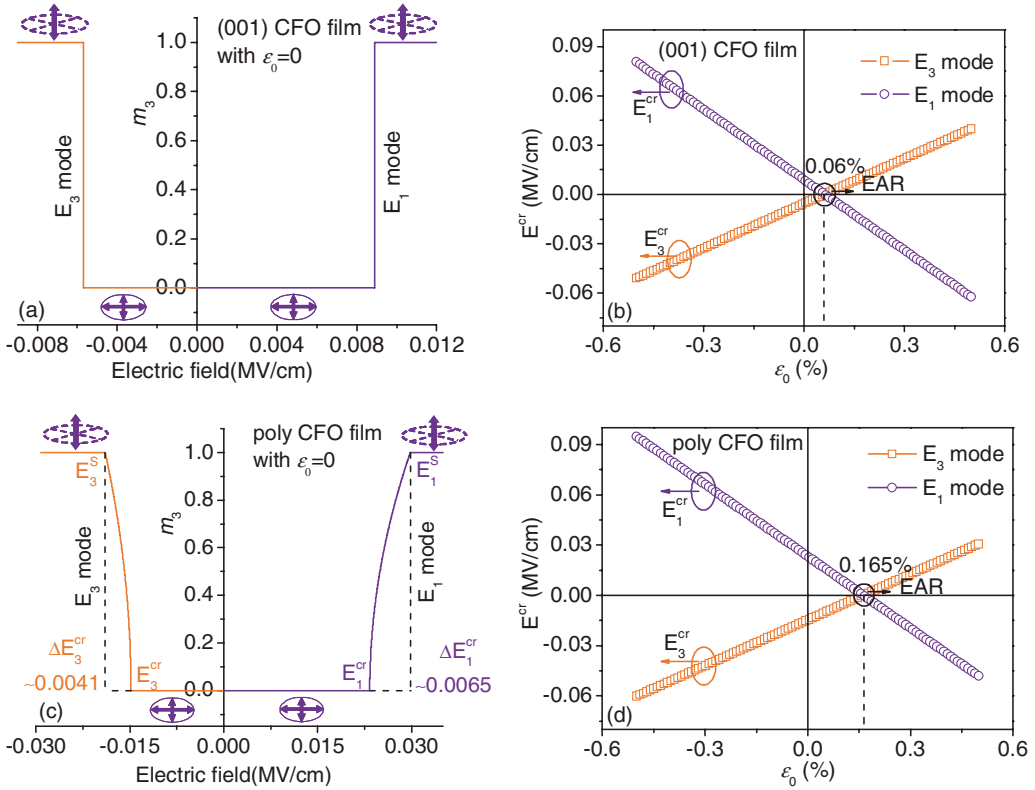

FIG. 4. (Color online) m_3 of the magnetic easy axis in (a) (001)-oriented and (c) polycrystalline CFO films as a function of electric field in the E_3 and E_1 modes at $\varepsilon_0=0$. Dependence of E^{cr} on ε_0 in the E_3 and E_1 modes in (b) (001)-oriented and (d) polycrystalline CFO films. The FE layer is PZN-PT. The arrows within ellipses denote the magnetic easy axis.

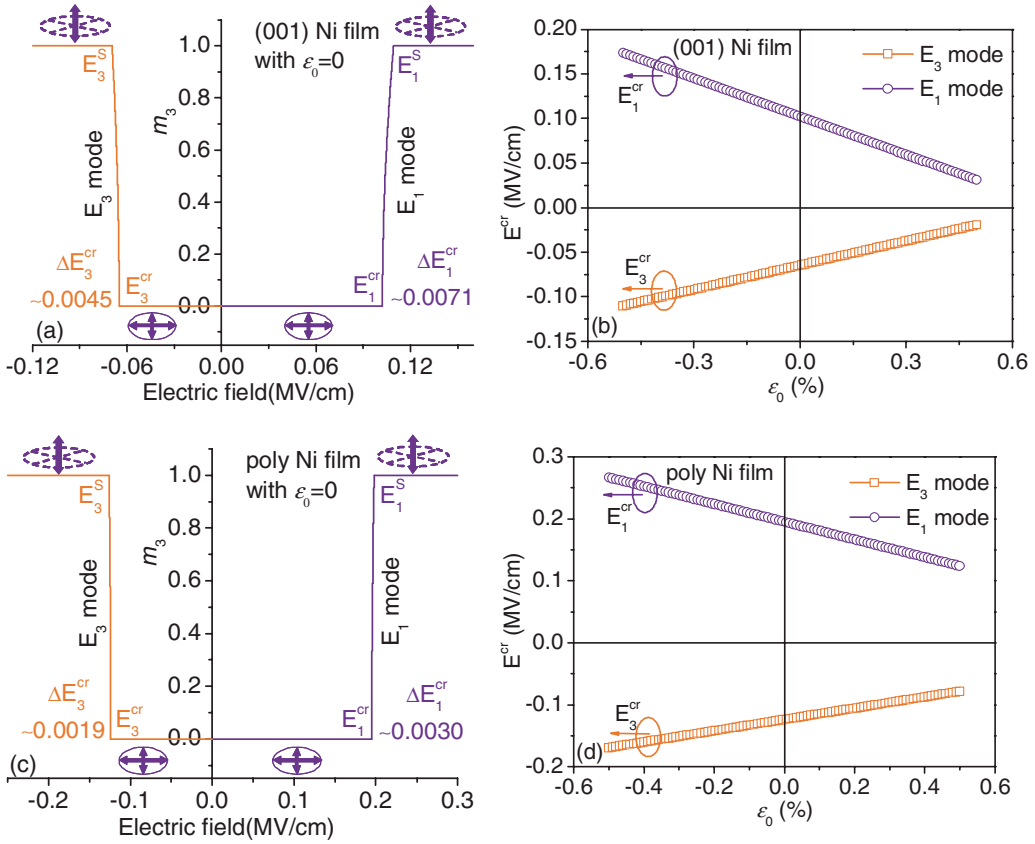

FIG. 5. (Color online) m_3 of the magnetic easy axis in (a) (001)-oriented and (c) polycrystalline Ni films as a function of electric field in the E_3 and E_1 modes at ε_0=0. Dependence of E^{cr} on ε_0 in the E_3 and E_1 modes in (b) (001)-oriented and (d) polycrystalline Ni films. The FE layer is PZN-PT. The arrows within ellipses denote the magnetic easy axis.

$$\Delta E_1^{cr} = E_1^S - E_1^{cr} = \frac{2K_B}{t(d_{31}+d_{33})}. \tag{19}$$

An applied electric field in this electric-field range can lead to the rotation of the magnetic easy axis. As shown in Fig. 4(c), ΔE_3^{cr} and ΔE_1^{cr} are 0.0041 and 0.0065 MV/cm, respectively, for the polycrystalline CFO film on PZN-PT at ε_0 =0. The influence of the residual strain ε_0 on the saturated electric field E_3^S (E_1^S) is the same as that on the critical electric field E_3^{cr} (E_1^{cr}), and greater in the E_1 mode as well [Fig. 4(d)]. As in the (001) CFO film, ε_0 has a similar effect on the critical electric field E_3^{cr} (E_1^{cr}) and the out-of-plane EAR happens at ε_0=0.165% where E_3^{cr} (E_1^{cr}) equals zero, as shown in Fig. 4(d).

From Table II and Fig. 4, one can see that E_3^{cr} and E_1^{cr} are −0.0057 and 0.0089 MV/cm for the (001) CFO films, −0.0148 and 0.0233 MV/cm for the polycrystalline CFO films, respectively, grown on a PZN-PT layer by assuming zero ε_0. If the BTO or PZT is used as the FE layer, the critical electric fields will be larger (see Table II). However, they can be reduced by a moderate positive ε_0. For example, E_3^{cr} of (001) CFO films on a BTO and PZT layer are −0.0158 and −0.0072 MV/cm at ε_0=0.05%, respectively. These values do not excess the coercive fields of the ferroelectric layers [e.g., $E_c \sim 0.025$ MV/cm (Ref. 19)]. Therefore, the electric-field-induced out-of-plane EAR is likely to happen in the CFO film owing to its low critical electric fields required, making it a promising candidate for the application in electric-write magnetic memories.

C. (001)-oriented and polycrystalline Ni and Fe_3O_4 films

Like polycrystalline CFO films discussed above, the Ni and Fe_3O_4 films present somewhat similar gradual rotation (i.e., second-order EAR) of the magnetic easy axes in a narrow electric-field range ΔE_3^{cr} or ΔE_1^{cr} (see Figs. 5 and 6) since they also exhibit positive K_B [i.e., about 5016 and 1118 J/cm^3 for (001) and polycrystalline Ni films; and 13420 and 788 J/cm^3 for (001) and polycrystalline Fe_3O_4 films, respectively]. Likewise, the sign and magnitude of the critical electric field E_3^{cr} (E_1^{cr}) and the saturated electric field E_3^S (E_1^S) can be obtained from Eqs. (14) and (16), respectively. ΔE_3^{cr} and ΔE_1^{cr}, determined from Eq. (19), are 0.0045 and 0.0071 MV/cm for the (001) Ni films, 0.0019 and 0.0030 MV/cm for the polycrystalline Ni films, respectively [see Figs. 5(a) and 5(c)]. These values are comparable to those for the polycrystalline CFO films, however, their E_3^{cr} (E_1^{cr}) and E_3^S (E_1^S) values are much larger than those for the CFO films.

Likewise, it is reasonable to limit our discussion on the critical electric field E_3^{cr} (E_1^{cr}) since the influences of ε_0 on the E_3^{cr} (E_1^{cr}) and E_3^S (E_1^S) are the same [see Eqs. (14) and (18)]. Such influences of ε_0 for the (001) and polycrystalline Ni films are shown in Figs. 5(b) and 5(d), respectively. A

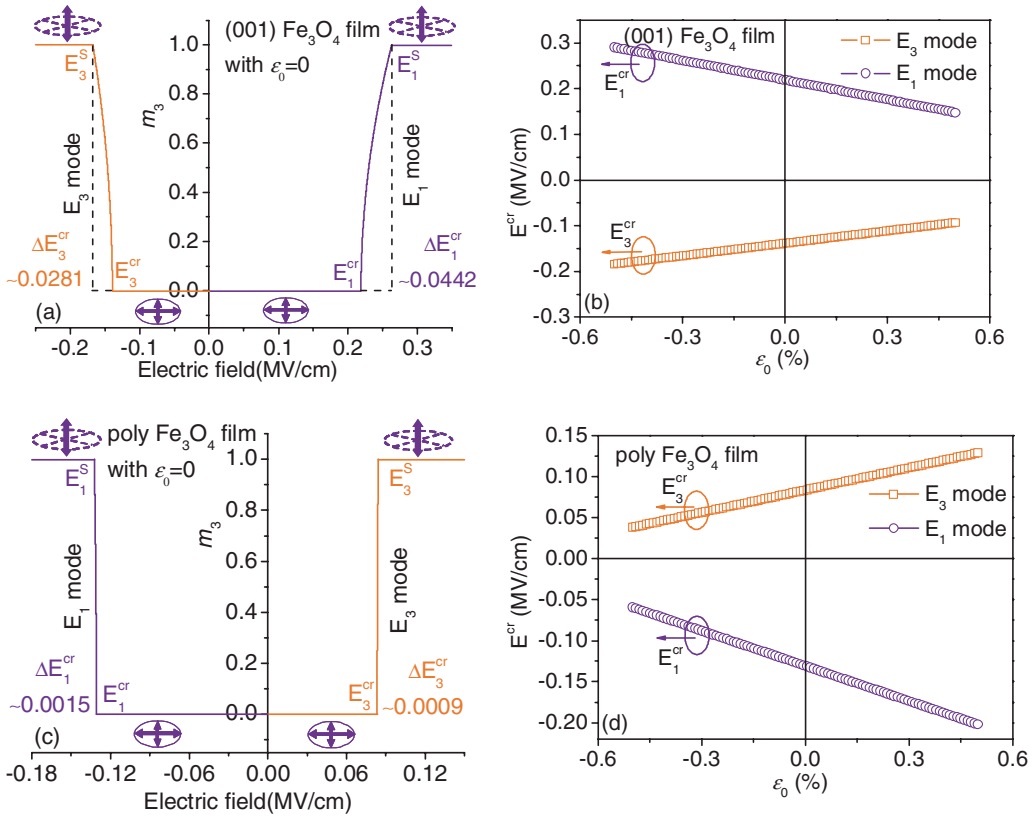

FIG. 6. (Color online) m_3 of the magnetic easy axis in (a) (001)-oriented and (c) polycrystalline Fe_3O_4 films as a function of electric field in the E_3 and E_1 modes at $\varepsilon_0=0$. Dependence of E^{cr} on ε_0 in the E_3 and E_1 modes in (b) (001)-oriented and (d) polycrystalline Fe_3O_4 films. The FE layer is PZN-PT.

positive ε_0 can reduce the critical electric fields [see Figs. 5(b) and 5(d)] but not enough to induce an out-of-plane EAR alone as in the case of the CFO films [see Figs. 4(b) and 4(d)]. For example, E_3^{cr} of the (001) Ni films with PZN-PT, PZT, and BTO layers at $\varepsilon_0=0.5\%$ are reduced to −0.0195, −0.1264, and −0.2755 MV/cm, respectively. Some of these values do not exceed their corresponding ferroelectric coercive fields ($E_c \sim 0.025$ MV/cm), which indicates the electric-field-induced out-of-plane EAR could be experimentally accessible in the Ni films. For (001) Ni film, Pertsev[14] presented a similar gradual electric-field-induced out-of-plane EAR.

Similarly, both the (001) and polycrystalline Fe_3O_4 films exhibit a gradual electric-field-induced out-of-plane EAR [see Figs. 6(a) and 6(c)] and the influences of the residual strain ε_0 on their critical electric fields E_3^{cr} (E_1^{cr}) are shown in Figs. 6(b) and 6(d), respectively, which can be interpreted in the same way as in the Ni films. However, the critical electric field E_3^{cr} (E_1^{cr}) is larger than the ferroelectric coercive field of the corresponding FE layers (see Tables II and III). Thus, an electric-field-induced out-of-plane EAR is difficult to be achieved in the Fe_3O_4 films.

D. Effect of nonlinear strain vs electric-field behavior

The in-plane strain does not always change linearly with the applied electric field E on the FE layer. Shown in Fig. 7(a) is a typical butterfly shaped strain-electric-field curve of

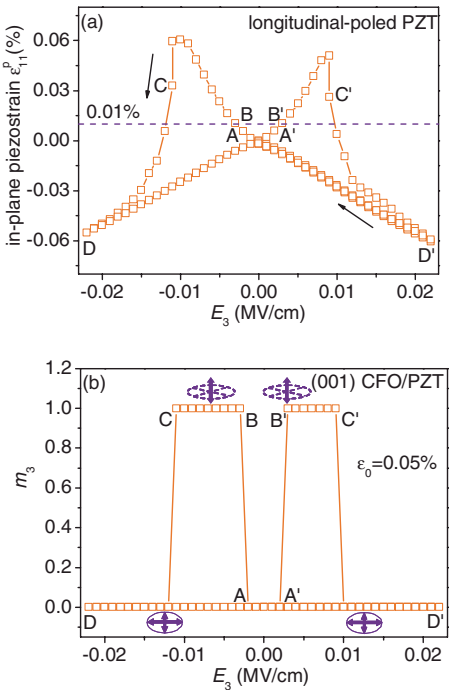

FIG. 7. (Color online) (a) In-plane piezostrains ε_{11}^p vs applied longitudinal electric field E_3 for a polarized PZT ceramic; the dashed lines indicates the smallest piezostrains required for the out-of-plane EAR in the (001) CFO films. (b) m_3 of the magnetic easy axis in the (001)-oriented CFO films at $\varepsilon_0=0.05\%$ as a function of E_3.

a longitudinal-polarized PZT ceramic recorded by a strain gauge upon a longitudinal electric field E_3. As shown in Fig. 7(a), when E_3 reaches the FE coercive field E_c, the in-plane piezostrain ε_{11}^p shows a strong nonlinear dependence on the electric field. Similar nonlinear strain vs electric-field behavior in other ferroelectrics has also been observed.[19] To demonstrate the influence of such nonlinear behaviors on the electric-field-induced out-of-plane EAR, the data of the in-plane piezostrains ε_{11}^p in Fig. 7(a) were introduced in our anisotropy model to calculate the total free-energy change ΔF_{tot}. Then the stable orientation of the magnetic easy axis can be determined also by minimizing ΔF_{tot}.

For illustration, we just take the (001)-CFO/PZT heterostructure as an example since the electric-field-induced out-of-plane EARs are more likely to happen in the (001)-CFO films as discussed above. Let us see the case under negative applied electric fields, i.e., from point A to D [see Fig. 7(a) and the same for the case from point A′ to D′]. As shown in Fig. 7(b), the magnetic easy axis in the (001) CFO/PZT heterostructure suddenly switches from the in-plane direction before the point A to the out-of-plane direction at point B (E_3^B=−0.003 MV/cm) and then flips back to the film plane abruptly at point C (E_3^C=−0.011 MV/cm). The reason for the transition is that the least piezostrain required for the out-of-plane EAR in the (001) CFO films is 0.01% as marked by the dashed line in Fig. 7(a). In consequence, the out-of-plane EAR happens only when $\varepsilon_{11}^p > 0.01\%$ (e.g., at points B and C) and the electric field E_3^B can be approximated as the critical electric field E_3^{cr}. After the point C, with the further increase in the negative E_3, ε_{11}^p gradually reduces to zero and reaches its negative maximum at the point D (E_3^D =−0.022 MV/cm) [see Fig. 7(a)] and the magnetic easy axis still lies in the film plane [see Fig. 7(b)] because the ε_{11}^p values are below the critical value 0.01%. Moreover, it can be seen from Fig. 7(b) that the out-of-plane EAR can also be induced by a positive E_3 field due to the symmetric behavior of strain-electric-field loop, different from previous results based on linear strain-electric-field relationship [Fig. 4(a)].

IV. ELECTRIC-FIELD-INDUCED IN-PLANE EAR

Compared with the out-of-plane EAR discussed above, an electric-field-induced in-plane EAR, i.e., an in-plane rotation of the magnetic easy axis induced by an electric field, more easily happens since no extra energy is needed for overcoming the large shape anisotropy energy. Still let us consider (001)-oriented and polycrystalline FM films. If the applied electric field is not high enough to induce an out-of-plane EAR ($E < E^{cr}$) then the magnetic easy axis lies in the film plane (see Fig. 2). In this case, the direction cosine m_3 in Eqs. (3)–(5) is zero and thus the total free-energy contribution can be expressed as

$$\Delta F_{tot} = K_1 m_1^2 (1 - m_1^2) - \frac{3}{2}\lambda_{100}(c_{11} - c_{12})(\varepsilon_{11} - \varepsilon_{22})m_1^2,$$

for epitaxial case, (20a)

TABLE IV. The critical electric fields E_1^{cr} for the electric-field-induced in-plane EAR in (001)-oriented FM films at ε_0=0 with PZN-PT, BTO, and PZT as the FE layers.

	E_1^{cr} (MV/cm)		
Films	PZN-PT	BTO	PZT
Fe	0.0389	0.5222	0.2413
CFO	−0.0028	−0.0373	−0.0172
Ni	−0.0014 ~ 0.0014	−0.0183 ~ 0.0183	−0.0084 ~ 0.0084
Fe_3O_4	−0.0063 ~ 0.0063	−0.0840 ~ 0.0840	−0.0388 ~ 0.0388

$$\Delta F_{tot} = -\frac{3}{2}\lambda_S(c_{11} - c_{12})(\varepsilon_{11} - \varepsilon_{22})m_1^2,$$

for polycrystalline case, (20b)

where those terms independent of the direction cosines were omitted. The critical in-plane electric field E_1^{cr} can thus be deduced as shown in Table IV.

For the longitudinal electric field E_3, we have $\varepsilon_{11} - \varepsilon_{22} = 0$ on the condition that the residual strains along two in-plane directions are equal and the FM/FE interface can pass the strains homogeneously. In this case, the electric field E_3 could not induce an in-plane EAR, which means the magnetic easy axis might not be able to rotate within the film plane upon a longitudinal electric field.

Comparatively, when the ferroelectric substrate is upon a transverse electric field E_1, it can be derived that

$$\varepsilon_{11} - \varepsilon_{22} = (d_{33} - d_{31})E_1 \tag{21}$$

according to Eq. (11). Thus Eqs. (20a) and (20b) could be further written as

$$\Delta F_{tot} = \left[K_1 - \frac{3}{2}\lambda_{100}(c_{11} - c_{12})(d_{33} - d_{31})E_1\right]m_1^2 - K_1 m_1^4,$$

for epitaxial case, (22a)

$$\Delta F_{tot} = -\frac{3}{2}\lambda_S(c_{11} - c_{12})(d_{33} - d_{31})E_1 m_1^2,$$

for polycrystalline case. (22b)

Likewise, the change in the easy axis could be described through the minimization of the total free energy. For (001)-oriented films, a critical transverse electric field E_1^{cr} is needed to overcome in-plane magnetocrystalline anisotropy and corresponding electric-field-induced in-plane EARs are shown in Fig. 8. Moreover, it can be seen from Eq. (22a) that the expression of the total free energy exhibits a quartic term with a coefficient $-K_1$. Similarly to Eq. (16), such an electric-field-induced in-plane EAR can be defined as a second-order EAR when $-K_1 > 0$ and a first-order one when $-K_1 < 0$ as discussed above. Thus, it can be concluded that the (001) Fe and CFO films show a first-order in-plane EAR ($K_1 > 0$, see Table I) at a critical transverse electric field E_1^{cr}, i.e.,

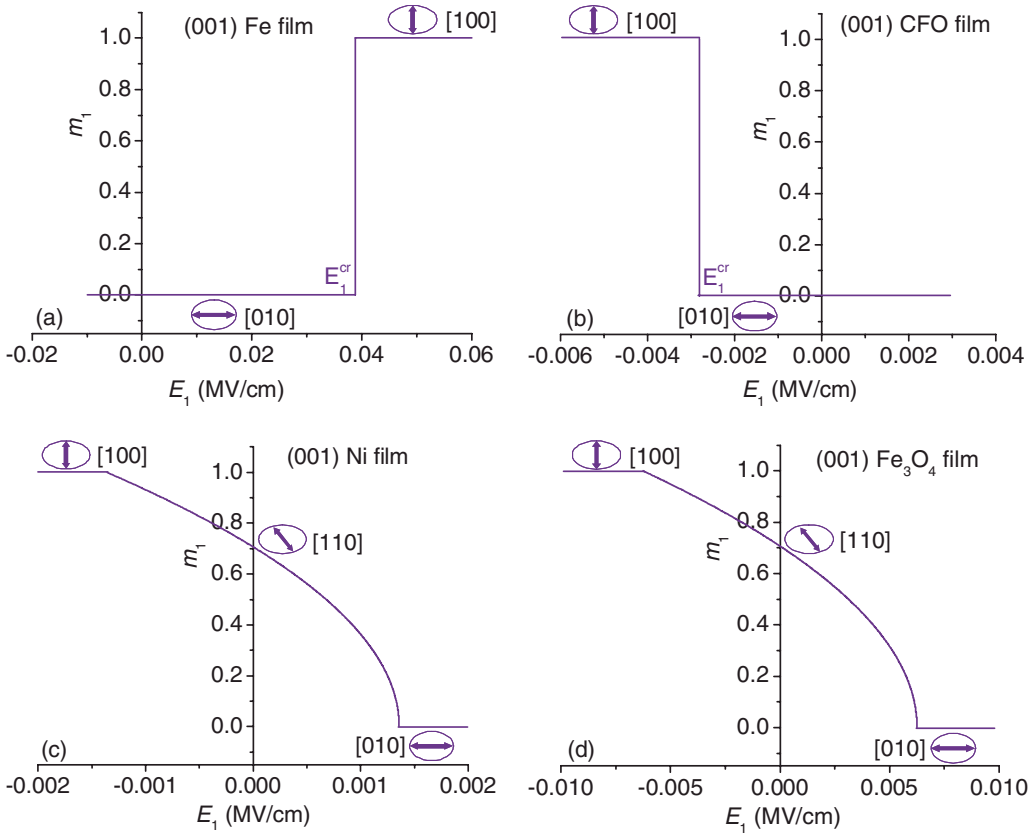

FIG. 8. (Color online) Electric-field-induced in-plane EAR: m_1 of the magnetic easy axis in (001)-oriented (a) Fe, (b) CFO, (c) Ni, and (d) Fe_3O_4 films as a function of a transverse electric field E_1 at $\varepsilon_0=0$. The arrows within ellipses denote the magnetic easy axis.

$$E_1^{cr} = \frac{2K_1}{3\lambda_{100}(c_{11}-c_{12})(d_{33}-d_{31})}. \tag{23}$$

The easy axis changes discontinuously at this critical point from an initial in-plane [010] direction where $m_1=0$, to another in-plane direction [100] where $m_1=1$, or vice versa, depending on the sign of the K_1/λ_{100} [see Figs. 8(a) and 8(b)].

For the (001) Ni and Fe_3O_4 films, a second-order in-plane EAR is expected ($K_1<0$, see Table I). In the (001) Ni film, the magnetic easy axis changes gradually from [100] to [010] within a certain range of transverse electric field E_1, i.e.,

$$-E_1^{cr} < E_1 < E_1^{cr}, \tag{24}$$

where $K_1<0, \lambda_{100}>0$. Likewise, in the (001) Fe_3O_4 film, we have

$$E_1^{cr} < E_1 < -E_1^{cr} \tag{25}$$

Figures 8(c) and 8(d) show such a second-order electric-field-induced in-plane EAR for the (001) Ni and Fe_3O_4 films, respectively. It is worth noting that the magnetic easy axes are along the direction [110] ($m_1=\sqrt{2}/2$) at $E_1=0$, which is reasonable in the respect that [110] is the projective direction of [111], i.e., the orientation of the magnetic easy axis, for instance, in bulk Ni single crystals, onto the (001) film plane.

As shown in Table IV, the transverse electric field E_1 can easily induce an in-plane EAR, where the values of E_1^{cr} are much smaller than those for an out-of-plane EAR. For example, in the (001) CFO, Ni, and Fe_3O_4 films, most of these E_1^{cr} are lower than their corresponding FE coercive fields, which indicates such electric-field-induced in-plane EARs could occur in these FM films. When the effect of the residual strain is taken into account, E_1^{cr} can be further reduced. These characteristics provide more degrees of freedom for engineering functionality into these ferromagnets.

For polycrystalline FM films, the critical electric field E_1^{cr} equals zero, which means that a 90° switching of the magnetic easy axis in the film plane can be produced just by changing the sign of the applied electric field. These results are in accordance with recent experimental observations in polycrystalline Ni films[9] and (001)-oriented epitaxial Fe_3O_4 films.[10]

V. CONCLUSIONS

The electric-field-induced easy-axis reorientation in FM/FE-layered heterostructures, i.e., the switch of the magnetic easy axis driven by an electric field applied to the FE layer, has been investigated systematically, based on a phenomenological approach. The FM layers include the widely used Fe, CFO, Ni, and Fe_3O_4 films, that are either polycrystalline or (001) preferentially oriented. For most cases, the magnitudes of the critical electric fields E^{cr} for the EAR in the (001)-oriented FM films are smaller than their polycrystalline counterparts. The relaxor ferroelectrics such as PZN-PT as well as normal ferroelectrics such as BTO and PZT are used

as the FE layers, and E^{cr} decreases with increasing piezoelectric coefficients.

Such electric-field-induced EARs are classified into an out-of-plane EAR and an in-plane one. The in-plane EAR could happen in CFO, Fe_3O_4, and Ni films at relatively low applied electric field, among which, the (001) Ni/PZN-PT heterostructure exhibits the lowest critical electric field (see Table IV) owing to the lowest K_1/λ_{100} ratio and large piezoelectric coefficients [see Eq. (23)]. As the applied electric field increases, the out-of-plane EAR is likely to be induced but only experimentally accessible in CFO and Ni films, which are limited by the dielectric breakdown field or the coercive field of corresponding FE layers. Among them, the (001) CFO/PZN-PT heterostructure shows the lowest critical electric fields (see Tables II and III) due to large magnetostrictive constants of CFO films as well as high piezoelectric coefficients of PZN-PT substrates.

Influences of different electric-field modes (i.e., a longitudinal E_3 mode and a transverse E_1 mode) on the EARs have been studied. It should be noted that the electric-field-induced in-plane EAR could only occur in the E_1 mode if the residual strains are deemed as equal in the film plane whereas the out-of-plane EAR could happen in both electric-field modes. The magnitudes of E_3^{cr} are lower than that of E_1^{cr}, which indicates the longitudinal electric field E_3 can induce the out-of-plane EAR more effectively. However, as the electric field E exceeds the ferroelectric coercive field E_c, nonlinear behavior of strain-electric-field relationship should be considered. Moreover, the critical electric fields can be greatly reduced by a careful control of the residual strain such as varying the thickness of FM layers and changing the thermal conditions during deposition process.

Both the electric-field-induced out-of-plane and in-plane EARs can be abrupt (discontinuous) or gradual (continuous), depending on the signs of the quartic coefficients in corresponding expressions of the total free energy. Such abrupt and gradual EARs are defined as the first-order and the second-order EARs, respectively.

ACKNOWLEDGMENTS

This work was supported by the NSF of China (Grant No. 50832003) and the National Basic Research Program of China (Grant No. 2009CB623303).

*Corresponding author. cwnan@tsinghua.edu.cn

[1] C.-W. Nan, M. I. Bichurin, S. Dong, D. Viehland, and G. Srinivasan, J. Appl. Phys. **103**, 031101 (2008).
[2] W. Eerenstein, N. D. Mathur, and J. F. Scott, Nature (London) **442**, 759 (2006).
[3] M. Liu, O. Obi, J. Lou, Y. J. Chen, Z. H. Cai, S. Stoute, M. Espanol, M. Lew, X. Situ, K. S. Ziemer, V. G. Harris, and N. X. Sun, Adv. Funct. Mater. **19**, 1826 (2009).
[4] W. Eerenstein, M. Wiora, J. L. Prieto, J. F. Scott, and N. D. Mathur, Nature Mater. **6**, 348 (2007).
[5] Y.-H. Chu, L. W. Martin, M. B. Holcomb, M. Gajek, S.-J. Han, Q. He, N. Balke, C.-H. Yang, D. Lee, W. Hu, Q. Zhan, P.-L. Yang, A. F. Rodriguez, A. Scholl, S. X. Wang, and R. Ramesh, Nature Mater. **7**, 478 (2008).
[6] I. Stolichnov, S. W. E. Riester, H. J. Trodahl, N. Setter, A. W. Rushforth, K. W. Edmonds, R. P. Campion, C. T. Foxon, B. L. Gallagher, and T. Jungwirth, Nature Mater. **7**, 464 (2008).
[7] D. Chiba, M. Sawicki, Y. Nishitani, Y. Nakatani, F. Matsukura, and H. Ohno, Nature (London) **455**, 515 (2008).
[8] C. Thiele, K. Dörr, O. Bilani, J. Rödel, and L. Schultz, Phys. Rev. B **75**, 054408 (2007).
[9] M. Weiler, A. Brandlmaier, S. Geprägs, M. Althammer, M. Opel, C. Bihler, H. Huebl, M. S. Brandt, R. Gross, and S. T. B. Goennenwein, New J. Phys. **11**, 013021 (2009).
[10] A. Brandlmaier, S. Geprägs, M. Weiler, A. Boger, M. Opel, H. Hubel, M. S. Brandt, R. Gross, and S. T. B. Goennenwein, Phys. Rev. B **77**, 104445 (2008).
[11] C.-G. Duan, S. S. Jaswal, and E. Y. Tsymbal, Phys. Rev. Lett. **97**, 047201 (2006).
[12] J. M. Rondinelli, M. Stengel, and N. A. Spaldin, Nat. Nanotechnol. **3**, 46 (2008).
[13] N. Mathur, Nature (London) **454**, 591 (2008).
[14] N. A. Pertsev, Phys. Rev. B **78**, 212102 (2008).
[15] L. D. Landau, E. M. Lifshitz, and L. P. Pitaevskii, *Electrodynamics of Continuous Media* (Pergamon, Oxford, 1984).
[16] A. Yamaguchi, S. Ogu, W.-H. Soe, and R. Yamamoto, Appl. Phys. Lett. **62**, 1020 (1993).
[17] E. du Trémolet de Lacheisserie, Phys. Rev. B **51**, 15925 (1995).
[18] B. D. Cullity, *Introduction to Magnetic Materials* (Addision-Wesely, Reading, MA, 1972).
[19] S.-E. Park and T. R. Shrout, J. Appl. Phys. **82**, 1804 (1997).
[20] J. Yin and W. Cao, J. Appl. Phys. **92**, 444 (2002).
[21] G. H. Haertling, J. Am. Ceram. Soc. **82**, 797 (1999).
[22] Y. Saito, H. Takao, T. Tani, T. Nonoyama, K. Takatori, T. Homma, T. Nagaya, and M. Nakamura, Nature (London) **432**, 84 (2004).
[23] A. Lisfi, C. M. Williams, L. T. Nguyen, J. C. Lodder, A. Coleman, H. Corcoran, A. Johnson, and P. Chang, Phys. Rev. B **76**, 054405 (2007).